

The CLAPPER: A Dual-drive Mobile Robot With Internal Correction of Dead-reckoning Errors

Johann Borenstein

The University of Michigan, MEAM Mobile Robotics Lab

ABSTRACT

This paper presents a new approach to accurate and reliable dead-reckoning with mobile robots. The approach makes use of special properties of our recently developed Multi-Degree-of-Freedom (MDOF) mobile platform, in which two differential-drive mobile robots (called "trucks") are physically connected through a compliant linkage. Using one linear and two rotary encoders, the system can measure the relative distance and bearing between the two trucks. During operation, both trucks perform conventional dead-reckoning with their wheel encoders, but, in addition, use information about their relative position to correct dead-reckoning errors.

Our system, called Compliant Linkage Autonomous Platform with Position Error Recovery (CLAPPER), requires neither external references (such as navigation beacons, artificial landmarks, known floorplans, or satellite signals), nor inertial navigation aids (such as accelerometers or gyros). Nonetheless, the experimental results included in this paper show one to two orders of magnitude better positioning accuracy than systems based on conventional dead-reckoning.

1. INTRODUCTION

In most mobile robot applications two basic position-estimation methods are employed together: absolute and relative positioning [Borenstein and Koren, 1987; Hongo et al, 1987]. Relative positioning is usually based on dead-reckoning (i.e., monitoring the wheel revolutions to compute the offset from a known starting position). Dead-reckoning is simple, inexpensive, and easy to accomplish in real-time. The disadvantage of dead-reckoning is its unbounded accumulation of errors.

Absolute positioning methods usually rely on (a) navigation beacons, (b) active or passive landmarks, (c) map matching, or (d) satellite-based navigation signals. Each of these absolute positioning approaches can be implemented by a variety of methods and sensors. Yet, none of the currently existing systems is particularly elegant. Navigation beacons and landmarks usually require costly installations and maintenance, while map-matching methods are either very slow or inaccurate

[Cox, 1991], or even unreliable [Congdon et al, 1993]. With any one of these measurements it is necessary that the work environment be either prepared or be known and mapped with great precision. Satellite-based navigation can be used only outdoors and has poor accuracy (on the order of several meters) when used in real-time, during motion.

Another approach to the position determination of mobile robots is based on inertial navigation with gyros and/or accelerometers. Our own experimental results with this approach, as well as the results published in a recent paper by Barshan and Durrant-Whyte [1993], indicate that this approach is not advantageous. Accelerometer data must be integrated twice to yield position, thereby making these sensors exceedingly sensitive to drift. Another problem is that accelerations under typical operating conditions can be very small, on the order of 0.01 g. Yet, fluctuation of this magnitude already occur if the sensor deviates from a perfectly horizontal position by only 0.5°, for example when the vehicle drives over uneven floors. Gyros can be more accurate (and costly) but they provide information only on the rotation of a vehicle.

This paper introduces a new method for correcting dead-reckoning errors without external references. This method requires two collaborating mobile robots that can accurately measure their relative distance and bearing during motion. Our previously developed MDOF vehicle [Borenstein, 1993; 1994a] meets these requirements and we were able to implement and test our error correction method on this vehicle with only minor modifications. Section 2 summarizes the relevant characteristics of our MDOF vehicle. Because of the new error correction capability, we now call our vehicle the Compliant Linkage Autonomous Platform with Position Error Recovery (CLAPPER). Section 3 describes the error correction method in detail, and Section 4 presents experimental results.

The advantage of MDOF vehicles over conventional mobile robots is that they can travel sideways and they can negotiate tight turns easily. However, existing MDOF vehicles have been found difficult to control because of their overconstrained nature [Reister, 1991; Killough and Pin, 1992]. These difficulties translate into severe wheel slippage or jerky motion under certain driving conditions. Because of this excessive wheel-slippage existing MDOF vehicles are not very suitable for mobile robot applications that rely heavily on dead-reckoning. Our MDOF vehicle overcomes these difficulties by introducing the *compliant linkage* design (Fig. 2). The compliant linkage accommodates momentary controller errors and thereby successfully eliminates the excessive wheel slippage reported by other makers of MDOF vehicles.

The schematic drawing in Fig. 2 shows the essential components of the compliant linkage vehicle. The vehicle comprises of two trucks (in our prototype, these are commercially available *LabMate* robots from TRC [1993]). The two trucks are connected by the compliant linkage, which allows force-free relative motion within its physical range. A linear encoder measures the momentary distance between the two trucks, and two absolute rotary encoders measure the rotation of the trucks relative to the compliant linkage. Each of the four drive wheels in the system has a shaft encoder to allow conventional dead reckoning.

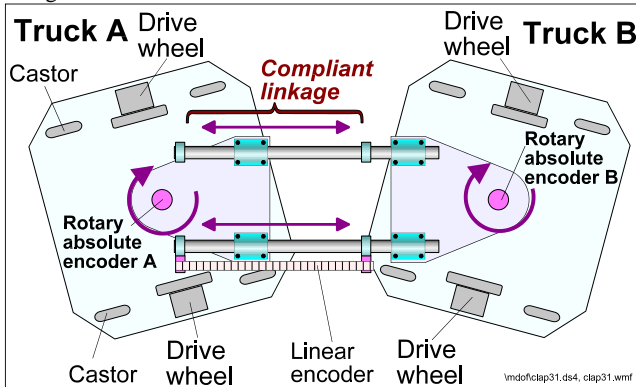


Figure 2: Essential components of the MDOF vehicle with compliant linkage.

The linear incremental encoder has a resolution of 0.1 mm, but the actual accuracy of distance measurements between the two trucks is only ± 5 mm because of mechanical inaccuracies in our prototype vehicle. The resolution of the rotary absolute encoders is 0.3° . We will call these the three "internal" encoders.

The experiments with our MDOF vehicle [Borenstein, 1993V1] showed that control errors are effectively absorbed by the compliant linkage, resulting in smooth and precise motion without excessive wheel slippage. In a series of 4×4 m square path experiments we found typical dead-reckoning errors to be less than 6.5 cm in x and y direction, and orientation errors were less than $\pm 1^\circ$ [Borenstein, 1994a]. This dead-reckoning accuracy is comparable with that of conventional 2-DOF robots. Of course, these results were obtained on smooth floors without irregularities, and with well calibrated parameters to minimize systematic errors.

3. INTERNAL CORRECTION OF DEAD-RECKONING ERRORS

At first glance, it may appear impossible to obtain accurate position corrections from a "floating reference point," such as another mobile robot *in motion*. Yet, our method is designed to overcome this problem: it exploits the fact that certain dead-reckoning errors develop slowly while others develop quickly. For example, when a robot traverses a bump or crack in the floor, it will experience an appreciable orientation error within just a few centimeters of travel ("fast-growing" error). The lateral position error, on the other hand, is very small at first ("slow-growing" error), although it will grow with distance as a function of the orientation error. Our method performs relative position measurements very frequently, allowing each truck to detect errors in its orientation (which can have changed significantly during one sampling interval), while relying on the fact that the lateral position error of both trucks was only small during the same interval.

Before we present the details of our method we should make a clear distinction between two types of dead-reckoning errors found in mobile robot navigation: (a) *systematic errors*, which are related to properties of the vehicle, that is, they are independent of the environment; and (b) *non-systematic errors*, which are usually caused by *irregularities* or roughness of the floor.

Note that non-systematic errors can neither be avoided nor can they be compensated for in conventional dead-reckoning. By contrast, the CLAPPER can detect and reduce both systematic and non-systematic errors by one to two orders of magnitude, even with both trucks in motion.

In this Section we explain our approach for the simple case of straight-forward motion, but the method works equally well (and without any modification) for curved trajectories. We will develop a numeric example throughout this section, to show why certain assumptions are valid.

At first, we assume that both trucks are longitudinally aligned and travel forward. For the sake of the numeric example, let us assume that both trucks are traveling at $V = 0.5$ m/s, and that the sampling time of the *internal encoders* is $T_s = 40$ ms. Thus, during a sampling interval both trucks travel a distance $D_s = VT_s = 20$ mm.

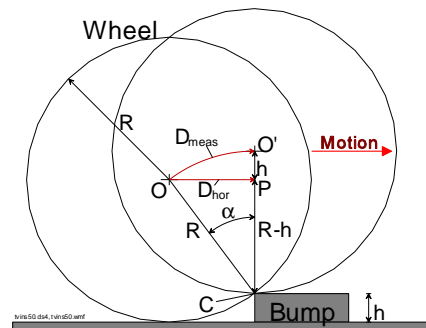


Figure 3: Simplified geometry of wheel traversing a bump.

Next, we consider the geometry of a wheel of radius R traversing a bump of height h (see Fig. 3). Making the simplifying assumption that the wheel was perfectly rigid, the wheel will

traverse the bump by rotating around the point of contact C until the wheel's center point O is right above C (at O'). During this motion the wheel encoder measures a rotation α , which is interpreted as the linear travel distance D_{meas} . Yet, the actual travel distance in *horizontal* direction is only D_{hor} . This discrepancy creates a linear error $\Delta D = 2(D_{meas} - D_{hor})$ (not shown in Fig. 3). Note that the factor '2' is used because the wheel travels up *and* down the bump.

For straight-line motion, the low-level controller of a conventional differential-drive mobile robot will try to keep the rotational velocities of both wheels equal. Thus, the *horizontal* distance traveled by the wheel that traversed the bump (let us assume it is the right wheel, in our example) will be ΔD less than that of the left wheel, causing a curved motion to the right, as shown in Fig. 4.

Applying simple geometric relations (based on Figs. 3 and 4, but not derived here in detail), the numeric sample results shown in Table I are obtained (all physical dimensions correspond to the *LABMATE* robot from TRC). We will use these sample numbers in the following discussion.

Table 1: Sample path errors after traversing a bump

<u>Physical Dimensions</u>	
Wheelbase b	340 mm
Wheel radius R	75 mm
Height of bump h	10 mm
<u>Computed Results</u>	
Linear error ΔD	2.63 mm
Orientation error $\Delta\theta_a$ (see Fig. 4)	44°
Lateral error after 10m travel $e_{lat}(D=10m)$	77 mm

The resulting orientation error $\Delta\theta_a$ (see Fig. 4) is the *most significant error* in the system [Feng et al, 1993], because it will cause an *unbounded* lateral error, e_{lat} which grows proportionally with distance at a rate of

$$e_{lat}(D) = D \cdot \Delta D / b = D \sin \Delta\theta_a \quad (1)$$

where

D - Distance traveled since clearing the bump

b - wheelbase

For example, Table I shows that the lateral error of truck A after only 10 m travel would be $e_{lat}(D=10\text{ m}) = 77\text{ mm}$.

The method for detecting dead-reckoning orientation errors is based on our new concept of *fast-growing* and *slow-growing* dead-reckoning errors. The CLAPPER performs relative position measurements very frequently, allowing each truck to detect *fast-growing* errors in its orientation (which can have changed significantly during one sampling interval), while

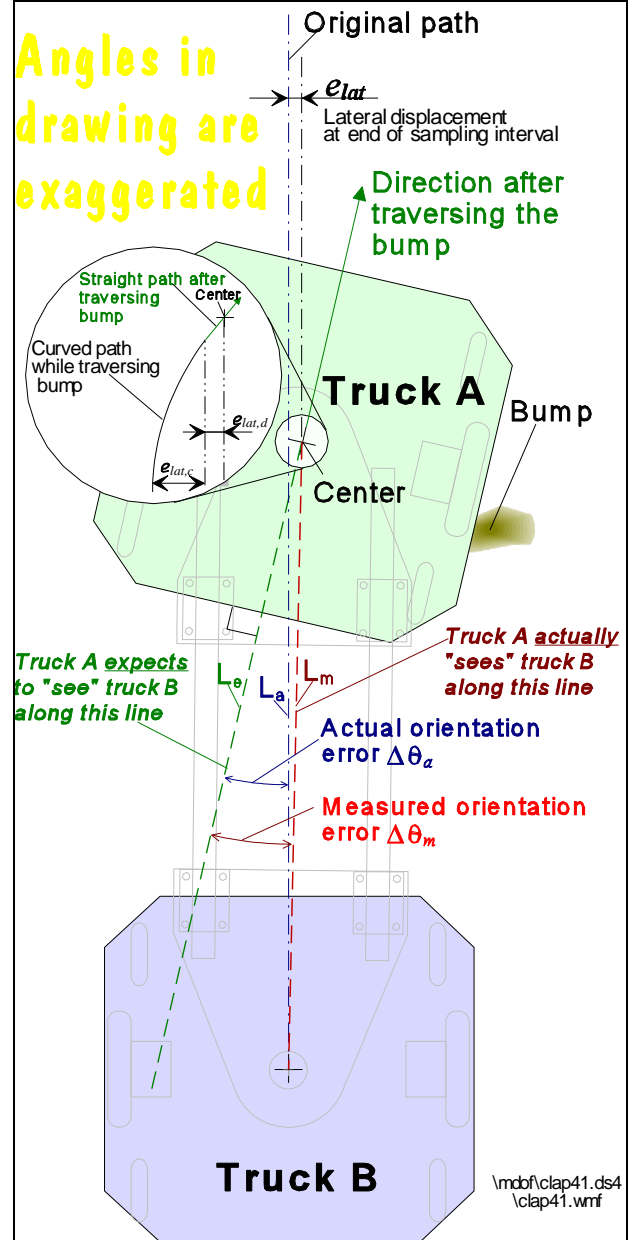


Figure 4: After traversing a bump, the resulting change of orientation of truck A can be measured relative to truck B.

The practical implementation of this approach works as follows: Figure 4 shows the direction in which truck A "expected" truck B, based on the dead-reckoning data from both trucks. If, however, truck A had traversed a bump, it would have acquired an orientation error $\Delta\theta_a$. Comparing the direction reading from absolute encoder A with the "expected" direction, the system can uncover this orientation error. Subsequently the internal world model of truck A can be corrected accordingly. One problem with this approach is the fact that even a perfectly accurate measuring system cannot reveal the actual orientation error $\Delta\theta_a$. Rather, because of the lateral offset e_{lat} the orientation error is measured

(incorrectly) as $\Delta\theta_m$. This allows us to correct the momentary orientation θ (based on dead-reckoning) in the internal world model of truck A by adding the measured orientation error $\Delta\theta_m$. The corrected orientation of truck A is therefore $\theta_{\text{corrected}} = \theta + \Delta\theta_m$.

In order to illustrate the validity of our approach we must show that the difference between $\Delta\theta_a$ and $\Delta\theta_m$ is indeed negligibly small under all normal driving condition. To do so, let us consider the enlarged area of Fig. 4. It is easy to compute the lateral position error $e_{\text{lat}}(D)$ after traversing the bump, because it increases at a constant rate as shown in Eq. (1). However, while traversing the bump the lateral position error changes as a function of the orientation error, which, in turn, is a function of the shape of the bump. Nonetheless, it can be shown that the orientation error increases monotonously while traversing a bump [Borenstein, 1994b]. Thus, any time we sample the orientation error $\Delta\theta_s$, we can be sure it is the largest orientation error from the time the bump was first encountered (i.e., $\Delta\theta_s \equiv \Delta\theta_{s,\text{max}}$). This holds true even if the wheel had not yet cleared the bump at the end of the sampling interval.

With this explanation in mind, an upper bound for the lateral orientation error while traversing a bump can be defined as

$$e_{\text{lat}}(D_s) \leq D_s \sin(\Delta\theta_s) \quad (2)$$

We recall that in our numeric example $D_s = 20$ mm and $\Delta\theta_s = 0.44^\circ$. Substituting these values into Eq. (2) yields $e_{\text{lat}}(D_s) = 0.15$ mm after traversing the bump.

Next, we can show that this lateral error has no significant influence on the accuracy of the relative orientation measurement between the two trucks. For example, the CLAPPER maintains a distance of $L = 1$ m between the two trucks. One can easily compute from the geometry of Fig. 4 that the small lateral error $e_{\text{lat}}(D_s) = 0.15$ mm will reduce the *actual* orientation error $\Delta\theta_a = 0.76^\circ$ by $\epsilon = \sin^{-1}(e_{\text{lat}}(D_s)/L) = \sin^{-1}(0.15/1000) = 0.01^\circ$ and result in a *measured* orientation error $\Delta\theta_m = \Delta\theta_a - \epsilon = 0.76^\circ - 0.01^\circ = 0.75^\circ$.

Thus, the lateral error e_{lat} does reduce the accuracy of the orientation error measurement, but only by $\epsilon = 0.01^\circ$, i.e., much less than the resolution of the *internal encoders*.

This numeric example illustrates how our approach exploits the concept of *slow-growing* and *fast-growing* dead-reckoning errors: Most floor irregularities will cause an appreciable, immediately measurable orientation error (*fast-growing* error), while the resulting lateral error e_{lat} remains negligibly small during the sampling interval (*slow-growing* error).

Figure 4 shows the simple case in which only truck A encountered a bump while truck B retained its heading. However, even in the worst case, (i.e., if truck B also encountered a bump during the same sampling interval), its lateral error $e_{\text{lat}}(D_s)$ would be similarly small. Neither this lateral error nor the orientation error of truck B would cause a significant error in the orientation measurement of truck A relative to B or vice versa. Yet, even in this extreme case, the inaccuracy of the orientation error measurement would only be $\epsilon = 2 \times 0.01^\circ = 0.02^\circ$, or $0.02/0.76 \times 100 = 2.6\%$.

The method described above can detect and reduce only rotational errors, but not translational errors. However, rotational errors are much more severe than translational errors, because orientation errors cause *unbounded* growth of lateral position errors. In the numeric example above, the translational error resulting from traversing a bump of height 10 mm was $\Delta D = 2.63$ mm. By comparison, the lateral error due to the rotational error $\Delta\theta$ is $e_{\text{lat}} = 77$ mm after only 10 m of further travel.

Another important strength of the CLAPPER's error correction system is the fact that *orientation errors do not accumulate*. This is so because the error correction (i.e., adding $\Delta\theta_m$ to the internal world model of truck A) is done in every sampling interval. Our experiments show that over-correction or under-correction in one sampling interval is simply "caught" in the next interval. Furthermore, it doesn't matter whether the discrepancy between expected and measured relative direction is the result of bumps, cracks, or systematic errors.

In principal the total orientation error of each truck is *bounded* by the resolution of the *internal encoders*. This is a major advantage compared to conventional dead-reckoning, where orientation errors do accumulate. In practice, however, our system cannot guarantee an error to be bounded by the encoder resolution. Our system is sensitive to systematic measurement errors from the encoders. For example, if rotary encoder A is constantly biased by, say, 0.5° , then the error correction function will assume a steady state in which truck A has a constant orientation error of 0.5° relative to the compliant linkage. Such an error would cause slightly curved motion of the CLAPPER (even on a perfectly smooth surface). Fortunately this systematic error can be detected experimentally and corrected by calibration with excellent results.

4. EXPERIMENTAL RESULTS

In order to evaluate the performance of the CLAPPER's error correction method we performed numerous sets of experiments.

In this paper we present the results of the basic *straight-line experiment*, where the CLAPPER was programmed to travel straight forward for 18 m, stop, and return straight-backward for 18 m, to the starting position.

In order to automate the evaluation of the experiments, all experiments started and ended near an L-shaped *reference corner*. Three ultrasonic sensors were mounted on the vehicle, two sensors were facing the long side of the L-shaped corner, the third sensor faced the short side. The ultrasonic sensor system allowed measurement of the absolute position of the vehicle to within ± 2 millimeters in the x and y directions, and to about $\pm 0.25^\circ$ in orientation.

At the beginning of each run a sonar measurement was taken to determine the starting position of the vehicle. The vehicle then traveled through the programmed path and returned to the L-shaped corner, where the *perceived* position (i.e., the position the vehicle "thought" it had, based on dead-reckoning) was recorded. Then, a sonar measurement was taken to determine the *absolute* position. The difference between the absolute position and the perceived position was the *position error*.

We performed three runs for each one of the following four conditions: (a) without error correction, without disturbances; (b)

without error correction, with disturbances; (c) with error correction, without disturbances; and (d) with error correction, with disturbances.

In the runs "without disturbances" one can assume disturbance-free motion because our lab has a fairly smooth concrete floor. In the runs "with disturbances" bumps were created by placing a 10 mm diameter cable placed under the wheels. We used bumps only on the return leg of the 2×18 m round-trip and only under the right-side wheels of the vehicle (to avoid mutual cancellation of errors). In the runs with error correction we used 20 bumps that were evenly spaced along the 18 m return-path. Some bumps affected both the front and rear truck, some affected only one of the two trucks. In the runs without error correction we used only 10 bumps, because our cluttered lab could otherwise not accommodate the large path deviations. Without error correction, each bump caused an orientation error of approximately 0.6° .

Figure 5 summarizes the results from the straight-line experiment. shown are the stopping positions and orientations of the vehicle after completing the 36 m journey back and forth along the x-axis. Each one of the four conditions of this experiment was performed three times. Note that without disturbances, the ending positions with error correction are only slightly better than those without correction. We relate the almost uniform error of approx. -1.7° in the run without error correction to systematic errors. The run with error correction shows how the systematic error is overcome. The more important results are those from runs with disturbances. Here the non-error corrected runs average -7.7° , out of which -1.7° are the result of the systematic error. The remaining error average of -6° were caused by applying identical 0.6° disturbances along the return path. Also note that the lateral position errors (without correction) would have been larger if the disturbances had been applied in the beginning of the return path.

We performed many more experiments than the ones documented here. In all runs the orientation error with the CLAPPER was less than $\pm 1.0^\circ$ for the 36 m path. The experiment described in this section, as well as several other experiments, are documented in the video proceedings of this conference [Borenstein, 1994V2].

5. ALTERNATIVE IMPLEMENTATIONS

We are currently investigating the possibilities of implementing our error correction method in a different kinematic configuration. This

configuration comprises only one differential drive mobile robot, which *tows* a small trailer with encoder wheels. Simulation results for this possible implementation indicate the feasibility of this approach [Borenstein, 1994c]. From a commercial point of view, the encoder trailer may be more attractive to manufacturers of mobile robots and AGVs, because the trailer can be attached to most existing vehicles.

6. CONCLUSIONS

The method described in this paper is applicable to many other autonomous vehicles. Vehicles used in construction or agricultural applications, where dead-reckoning has been impossible in the past because of the large amount of slippage on soft soil, may benefit directly from our new method. Furthermore, it may be possible to expand the *growth-rate concept* to tracked vehicles (like tanks or bulldozers) and possibly even to those watercraft and aircraft that have significantly different growth-rates in their positioning errors.

These features are made possible by exploiting the new concept of *growth-rate* of dead-reckoning errors that is introduced in this paper for the first time. The growth-rate concept distinguishes between certain dead-reckoning errors that develop

slowly while other dead-reckoning errors develop quickly. Based on this concept, truck A frequently measures a property with *slow-growing* error characteristics on reference truck B (thus admitting a small error) to detect a *fast-growing* error on truck A (thus correcting a large error), and vice versa.

In summary, the advantage of the CLAPPER system are:

1. The *immediate* correction of orientation errors, which would otherwise cause unbounded growth of lateral position errors.
2. Prevention of accumulation of orientation errors, to the limit determined by the calibration of the internal position measurement accuracy, and provided that none of the wheels slipped sideways.

Acknowledgements:

This research was funded by NSF grant # DDM-9114394 and in part by the Department of Energy. Special thanks to Dr. Liquiang Feng who provided comments and suggestions in the review of this manuscript.

7. REFERENCES

1. Barshan, B. and Durrant-Whyte, H.F., 1993, "An Inertial Navigation System for a Mobile Robot."

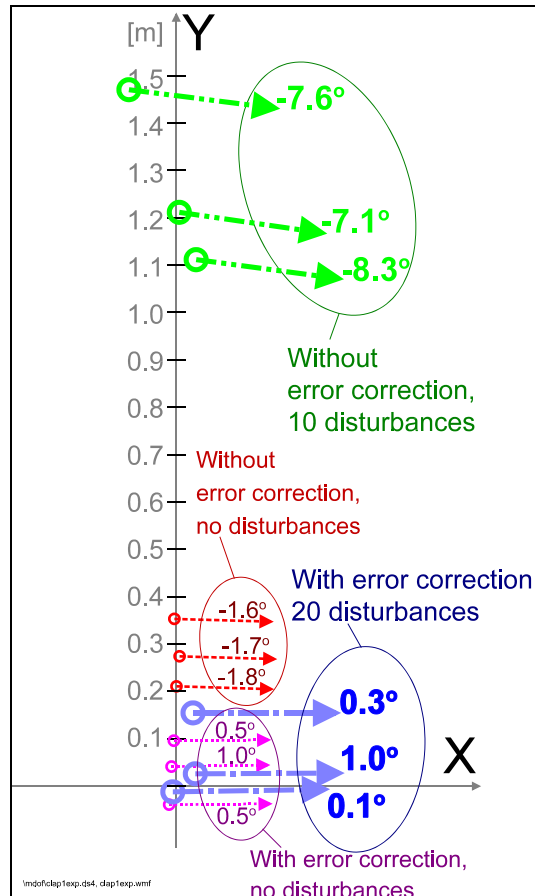


Figure 5: CLAPPER stopping positions after completing the straight-path experiment.

- Proceedings of the 1st IAV*, Southampton, England, April 18-21, 1993, pp. 54-59.
2. Borenstein, J. and Koren, Y., 1985, "A Mobile Platform For Nursing Robots." *IEEE Transactions on Industrial Electronics*, Vol. 32, No. 2, pp. 158-165.
 3. Borenstein, J. and Koren, Y., 1987, "Motion Control Analysis of a Mobile Robot." *Transactions of ASME, Journal of Dynamics, Measurement and Control*, Vol. 109, No. 2, pp. 73-79.
 4. Borenstein, J., 1993, "Multi-layered Control of a Four-Degree-of-Freedom Mobile Robot With Compliant Linkage." *Proceedings of the 1993 IEEE International Conference on Robotics and Automation*, Atlanta, Georgia, May 2-7, pp. 3.7-3.12.
 5. Borenstein, J., 1994a, "Control and Kinematic Design for Multi-degree-of-freedom Mobile Robots With Compliant Linkage." Conditionally accepted for publication (pending revisions) in the *IEEE Transactions on Robotics and Automation*, August 1993.
 6. Borenstein, J., 1994b, "Internal Correction of Dead-reckoning Errors With the Compliant Linkage Vehicle." Submitted for publication to the *Journal of Robotic Systems*, January 1994.
 7. Borenstein, J., 1994c, "Internal Correction of Dead-reckoning Errors With the Smart Encoder Trailer." Submitted to the *International Conference on Intelligent Robots and Systems (IROS '94)- Advanced Robotic Systems and the Real World*. September 12-16, 1994, Muenchen, Germany
 8. Borenstein, J., 1994V1, "Four-Degree-of-Freedom Redundant Drive Vehicle With Compliant Linkage." Submitted for inclusion in the *Video Proceedings of the 1994 IEEE International Conference on Robotics and Automation*, San Diego, CA, May 8-13, 1994.
 9. Borenstein, J., 1994V2, "The CLAPPER: A Dual-drive Mobile Robot With Internal Correction of Dead-reckoning Errors." Submitted for inclusion in the *Video Proceedings of the 1994 IEEE International Conference on Robotics and Automation*, San Diego, CA, May 8-13, 1994.
 10. Congdon, I. et al., 1993, "CARMEL Versus FLAKEY — A Comparison of Two Winners." *AI Magazine Winter 1992*, pp. 49-56.
 11. Cox, I. J., 1991, "Blanche — An Experiment in Guidance and Navigation of an Autonomous Robot Vehicle." *IEEE Transactions on Robotics and Automation*, vol. 7, no. 2, April, pp. 193-204.
 12. Feng, L., Koren, Y., and Borenstein, J., 1993, "A Cross-Coupling Motion Controller for Mobile Robots." *IEEE Journal of Control Systems Magazine*. December pp. 35-43.
 13. Killough, S. M. and Pin, F. G., 1992, "Design of an Omnidirectional Holonomic Wheeled Platform Prototype." *Proceedings of the IEEE Conference on Robotics and Automation*, Nice, France, May 1992, pp. 84-90.
 14. Hongo, T., Arakawa, H., Sugimoto, G., Tange, K., and Yamamoto, Y., 1987, "An Automated Guidance System of a Self-Controlled Vehicle." *IEEE Transactions on Industrial Electronics*, Vol. IE-34, No. 1, 1987, pp. 5-10.
 15. Reister, D. B., 1991, "A New Wheel Control System for the Omnidirectional HERMIES-III Robot." *Proceedings of the IEEE Conference on Robotics and Automation* Sacramento, California, April 7-12, pp. 2322-2327.
 16. TRC (Transition Research Corp), Shelter Rock Lane, Danbury, Connecticut, 06810.